Bull. Chem. Soc. Ethiop. **2023**, 37(6), 1459-1470.
DOI: https://dx.doi.org/10.4314/bcse.v37i6.13

ISSN 1011-3924
Printed in Ethiopia
Online ISSN 1726-801X

ANALYSING THE ROLE OF A BIO-SURFACTANT EXTRACTED FROM *COLOCASIA ESCULENTA* (L.) *SCHOTT* ON THE STABILIZATION OF HIGH CONCENTRATED IRON ORE SLURRY FOR TRANSPORTATION

Subrata Narayan Das[1,2], Susanta K. Biswal[1*], Ranjan K. Mohapatra[3*]

[1]School of Applied Sciences, Centurion University of Technology and Management, Odisha, India
[2]Department of Mining Engineering, Government College of Engineering, Keonjhar, Odisha, India
[3]Department of Chemistry, Government College of Engineering, Keonjhar, Odisha, India

(Received April 19, 2023; Revised July 20, 2023; Accepted August 4, 2023)

ABSTRACT. The transportation of minerals/ores in form of slurry through pipelines is an alternative, effective and also eco-friendly mode of transportation. Surfactants extracted from the plant sources are gaining high interest for the formulation and stabilization of high concentrated solid-water slurries. In this work, the role of a novel bio-surfactant extracted from *Colocasia esculenta* (L.) Schott on the stabilisation of iron ore slurry (IOS) was studied and reported first time. The collected iron ore powder (IOP) and dried IOS samples were analysed with the help of XRF, XRD, SEM and EDS analysis. The results confirmed that the surfactant molecules (present in aqueous *Colocasia esculenta* (L.) Schott) coated well on iron surface and forms an effective barrier between the iron ore (IO) particles. The studied rheological parameters for the slurry indicated non-Newtonian flow behaviour.

KEY WORDS: Iron ore **s**lurry, *Colocasia esculenta* (L.) Schott, XRD, SEM, rheological measurements

INTRODUCTION

As the steel industries are growing exponentially worldwide, and to meet the demand the iron ore is normally transported by rail and by road (truck and lorry). Such transportation system causes serious environmental pollutions due to particulate matters [1-3]. The rail and road transport has several impacts on the environment and ecosystem like air pollution, climate change, and noise pollution and further associated with health risks [1]. In addition to these impacts, such transport system has also other severe impacts on society. Moreover, for transporting the ores through the vehicles (trucks and lorries) that run in township crowed areas is life threatening. Every year thousands of people are killed and injured in accidents. Furthermore, increased International road and rail transport may impact severely. Transport related environmental pollution has many faces, but two are most important: emission of harmful compounds and vibroacoustic effects [1]. Further, such type of transportation makes chances of spillage of iron ore. Effective counteracting strategies in designing sustainable transport systems are highly recommended. Hence, the transportation of iron ore as slurry through pipelines is an alternative, economic and environmentally friendly transportation system which will overcome the congested transportation networks [4, 5].

Basically, the pipeline transportation system is widely used for the transportation of fluids such as petroleum and natural gas. But for solids with high specific gravity, need some changes in pipeline design may be due to abrasive nature. Slurry flow is used to transport solid particles with liquid (mostly water) as a carrier fluid. Slurry flow in pipelines is different from the single phase flow. The flow of slurry depends on the physical characteristics of the slurry and many factors such as concentration of solids in liquid phase, size and distribution of particles, and

*Corresponding author. E-mail: ranjank_mohapatra@yahoo.com ; dr.skbiswal@cutm.ac.in

viscosity of the carrier [6]. In high solid concentration and due to increase in particle-particle interaction, the viscosity of the slurry increases and ultimately affects the power requirements for pumping during the pipeline transportation of slurry [7]. This recommends special importance for the rapid and inexpensive means of formulating and stabilising the slurry [8].

Surfactants reduce the surface tension of water when mixed due to their amphiphilic nature. The commercial surfactants such as SDS, CTAB, etc. were used to stabilize different slurries. However, the stability and flowability of IOS by using the natural surfactants such as *Acacia auriculiformis* [9], *Sapindus mukorossi* [10], *Sapindus laurifolia* [11] and *Acacia concinna* [12] fruit extract was also reported recently. In our previous studies, we have successively used several bio-surfactants for the stabilisation of fly ash, and coal slurries [13-17]. In this present work, the rheological behaviour of a high grade IO slurry with concentration range of 50–70% by mass with a bio-surfactant (Figure 1) extracted from *Colocasia esculenta* (L.) Schott have been studied.

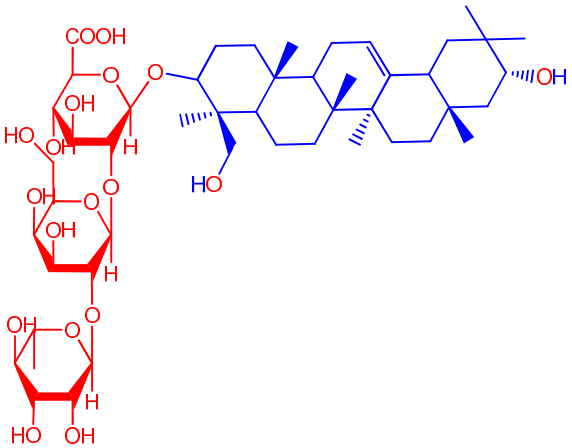

Figure 1. Structure of saponin molecule.

EXPERIMENTAL

Preparation of iron ore (IO) sample

The collected IO lumps obtained from Jindal Steel situated in Keonjhar district of Odisha, India, was crushed and powdered in the mineral engineering laboratory of Government College of Engineering (GCE), Keonjhar by using Jaw crusher (Testmaster) and ball mill with variable speed (Testmaster). The powdered IO was made to different sizes (-38 μm, +38-63 μm, +63-75 μm) with the help of standard sieves. As per the PSD (particle size distribution) analysis, the mean diameter of the collected IO sample is 8.11 μm with specific surface area 0.2633 m^2g^{-1}.

Preparation of aqueous extract of Colocasia esculenta (L.) Schott

Colocasia esculenta (L.) Schott is native to India, Bangladesh, China, Laos, Malaya, Myanmar, Nepal, Sumatera, Taiwan, Thailand. It is a tuberous geophyte and grows normally in the wet tropical biome. It is commonly used as food (root vegetable) for both animals and humans. In India, it is called 'Taro' and is one of the most ancient cultivated plants. *Colocasia esculenta* (L.) Schott commonly found in Odisha having very long coastal lines and inline water biomasses. Also this species is available in most part of the world having such agroclimatic conditions. We are

using *Colocasia esculenta* (L.) Schott leaf which is otherwise an organic waste with no other value added applications. As it is the waste by-product of saru, so it is cost effective and economical as compared to synthetic surfactants such as SDS, CTAB, etc. The *Colocasia esculenta* (L.) Schott leaf contains highest concentration of saponin. 100 g of the powdered leaves of *Colocasia esculenta* (L.) Schott was dissolved in 1L H_2O with the help of a magnetic stirrer. The resulting solution was filtered and used as a dispersant for the preparation of IO slurry. The CMC of *Colocasia esculenta* (L.) Schott was also analysed.

Measurement of rheological behavior

Desired concentration of the IO slurry was obtained by the addition of IO powder to a beaker having aqueous solution of *Colocasia esculenta* (L.) Schott with stirring for 20 min. The Rheological measurements of the IO slurry (concentration range of 50–70%) were carried out with the help of HAAKE RheoStress 1 (ThermoFisher). For rheological study, 30 mL of the slurry was introduced to a clean rheology cup under controlled shear rates (0 to 300 s^{-1}) with temperature 30 ℃.

Methods

The particle size distribution (PSD) of the collected IO sample was measured by using a Malvern Mastersizer instrument (Malvern, UK). The chemical composition of IO was analyzed with the help of Zentium, Malvern Panalytical. The X-ray diffraction (XRD) analysis was carried out with Bruker D8 advance XRD system. The surface morphology was studied from SEM and EDS analysis by using JEOL JSM-6480LV scanning electron microscope.

RESULTS AND DISCUSSION

X-ray fluorescence (XRF) study

The major component of the studied IO sample is hematite (Fe_2O_3) as observed from XRF analysis. The IO sample also contains very little amount of silica (SiO_2), alumina (Al_2O_3), P_2O_5, CaO along with some other compounds. The XRF analysis also suggests that the weight percentage of Fe_2O_3 slightly increased (97.57%) after the treatment with the surfactant [9].

SEM and EDS analysis

The surface morphology of the studied IO sample shows a well-formed structure, shape and texture with visible grains in microscales (Figure 2a). The SEM images presented various shapes ornamental and lacy grains with wide distribution. As observed, the grains are densely packed with low porosity over the surface of the IO sample. The nature of grains observed in these micrographs is suggested to be polycrystalline [9]. No change in the grains was observed after adding surfactant to the IO sample. The area scan EDS pattern of the IO sample confirmed the presence of iron 65.24% along with the oxygen 33.11% and silicon 0.72% (Figure 2b). The morphology of the surfactant treated IO can be observed in the Figure 2c. Well distributed and dense structure is observed on the surfactant treated IO particles. EDS shows the presence of 39.28 % silicon along with the iron and oxygen (Figure 2d). Figure 2e-f shows the presence of minute amount of Al at the marked region. Along with the major elements (Fe, O, Si, Al), the presence of C and Br can be found which is may be due to the presence of surfactant.

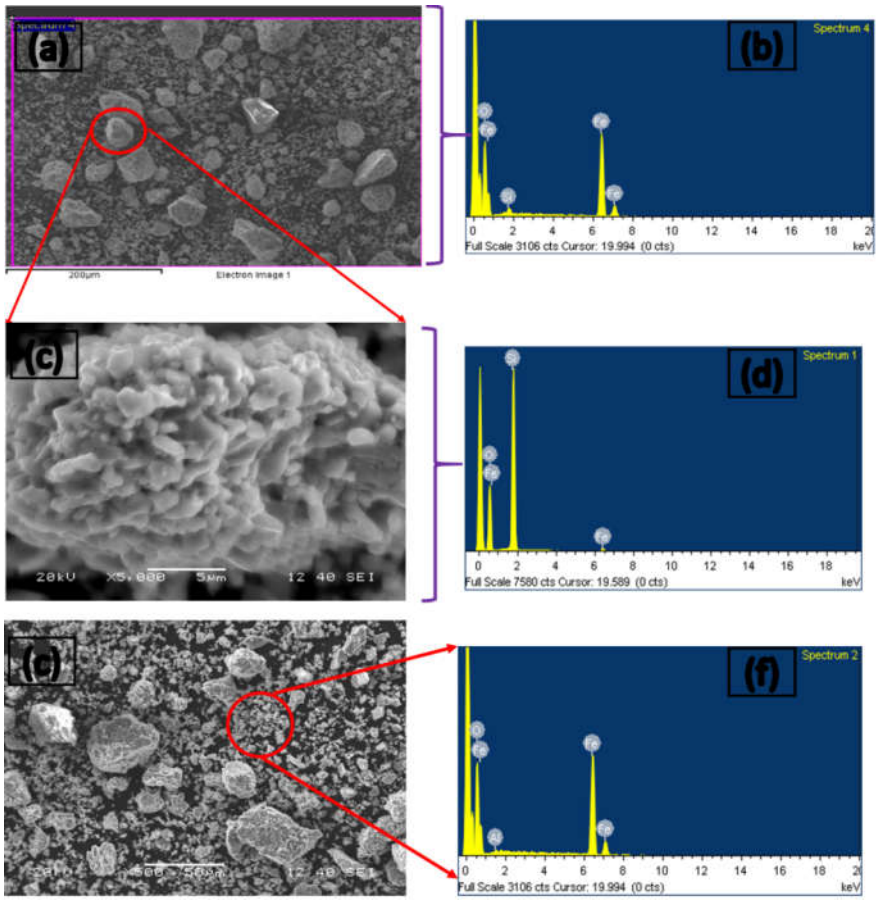

Figure 2. SEM and EDS pattern of the IO sample after treatment with the surfactant

XRD study

Figure 3 shows the phase analysis of the IO sample treated with the surfactant. The fine and intense peaks reflects a structural order in the compound and explains the existence of crystalline regions. The rhombohedral crystal structure with R-3c space group is identified from the XRD pattern by using the X'pert High score software. The lattice parameters of the selected unit cell were determined and given in the below Table 1.

Table 1. Lattice and structural parameters of IO samples.

Samples	a = b (A^0)	c(A^0)	Crystallite size (nm)	Dislocation density (nm^{-2})	Micro strain (ε)
IO sample (JCPDS 01-084-0307) [9]	5.6916	13.722	31.7	0.001321	0.0025
IO after treated with surfactant (JCPDS 01-084-0308)	5.0142	13.6733	27.6	0.001313	0.010

The size of crystallite (P) was approximately determined using Scherer's equation, $D = K\lambda/\beta_{1/2}\cos\theta_{hkl}$, (K is dimensionless shape factor which is nearly equal to 0.89, λ is X-ray wavelength of 1.5405Å and $\beta_{1/2}$ is peak width of the broadening line of XRD peak at half of the intensity) and the average value of P was determined as 27.6 nm which is comparatively smaller than the IO sample before treated with the surfactant. Thus, by treating IO with the surfactant, the crystallite size decreases.

According to Williamson and Hall, the crystallite size and microstrain are related to each other by equation, $\beta_{hkl} = \frac{K\lambda}{D} + 4\varepsilon\sin\theta$. The micro strain, and dislocation density of the sample were determined from the linear fitting, i.e. slope of Williamson-Hall Plot (β Cosθ vs Sinθ). Lower values of micro strain and dislocation density confirmed the smaller number of lattice defects which are given in Table 1.

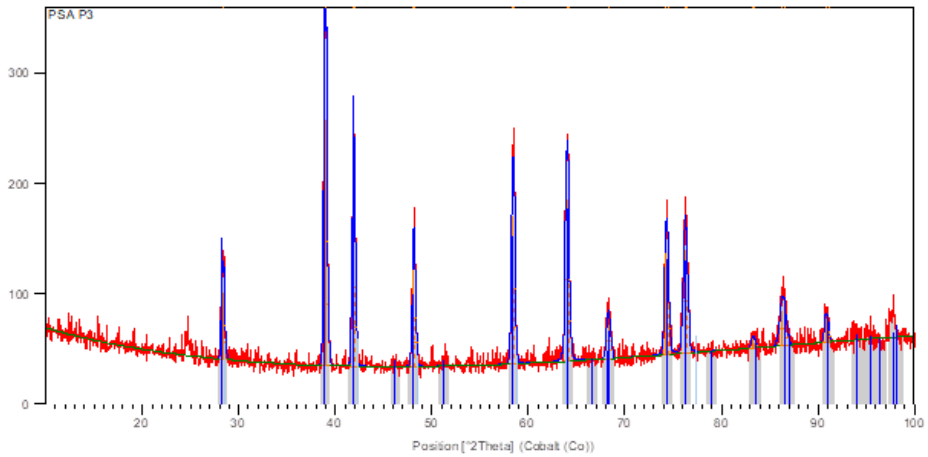

Figure 3. XRD pattern of the IO sample after treatment with the surfactant.

*DFT assessed descriptions of compound **1** (saponin)*

We have successfully optimized the compound **1** by using Gaussian16 suite of programs [18] at M06-2X/6-31G(d,p) method [19]. The optimized structure is shown in Figure 4(a). Further, the MEP surface analysis has been done to distinguish the reaction sites of the titled compound and to fully describe the regions of both electrophilic and nucleophilic attack. It is the pictorial method to realize the distribution of electron density in space around any molecule. [20-22] MEP uses many color descriptions, including orange, red, yellow, blue, and green. The red, orange, yellow, green, and blue are the colors in which the charge contribution decreases consistently, with deep red denoting negative potential and deep blue denoting positive potential. For this compound, we have found the molecular charge distribution in the range of $-8.124e^{-2}$ to $8.124e^{-2}$. Furthermore, the intense red color regions found around the oxygen atoms of carboxylic group while blue color regions at the methyl hydrogen atoms (Figure 4(b)).

Furthermore, as we know that, in the frontier molecular orbitals (FMOs), HOMO tends to donate electrons whereas the LUMO has the tendency to accept them. The energy gap (ΔE) of FMOs has direct relation with the kinetic stability and the chemical reactivity of any compound. [20,21] We have also computed the FMOs composition and calculated the energy gap of 6.14 eV. In addition, we have found that in HOMO most of the electron density present at the p_x/p_y orbitals of C=C whereas in LUMO the electron density available at the C=O carboxylic moiety (Figure 4(c)).

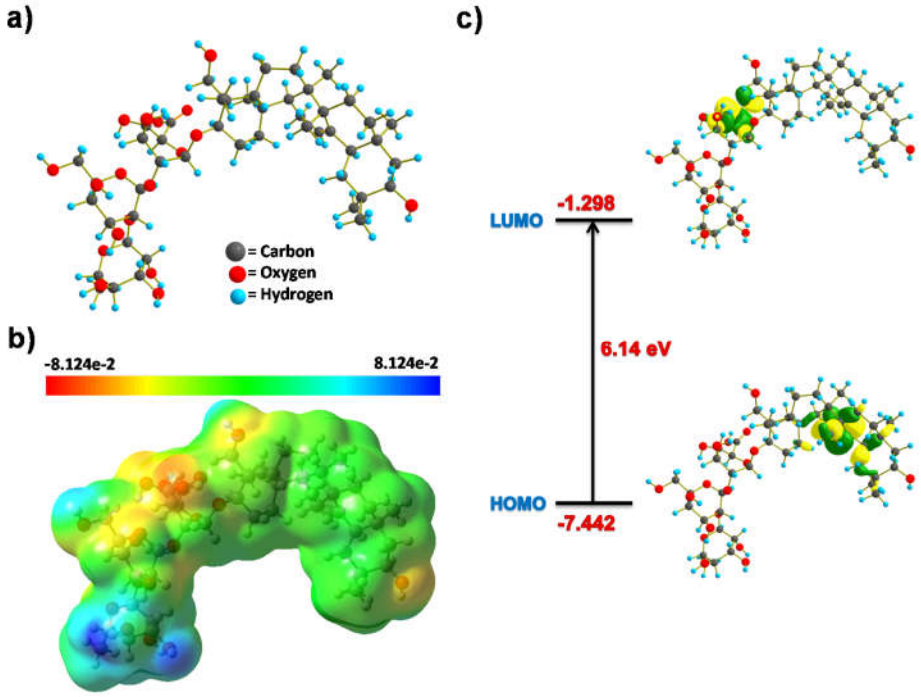

Figure 4. M06-2X/6-31G(d,p) optimized **a**) structure, **b**) MEP surface, and **c**) FMO composition of compound **1**.

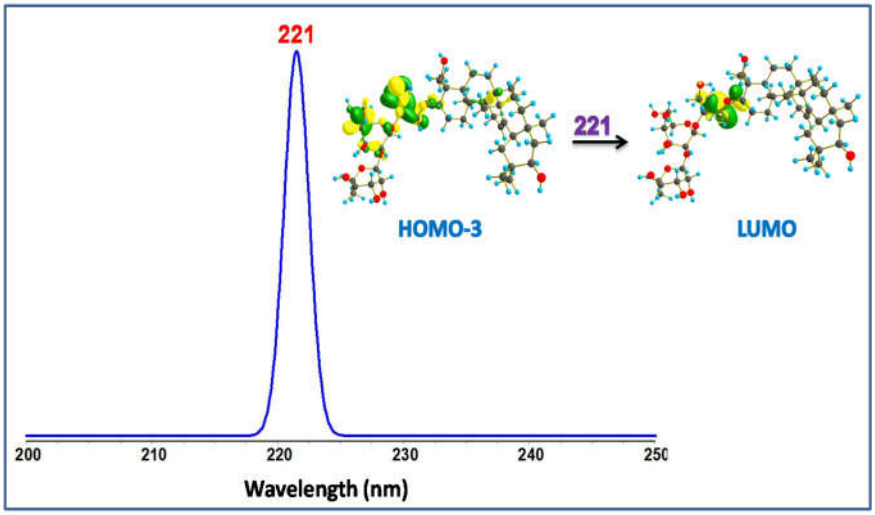

Figure 5. TD-DFT simulated absorption spectra of compound **1**.

TD-DFT studies

To explore the absorption spectrum of saponin molecule, we have done the TD-DFT calculation using ORCA 4.2 software [23]. Afterwards, in this molecule, we have found only one single peak in the ultraviolet (UV) region at 221 nm (Figure 5) which is found responsible for the $\pi \rightarrow \pi^*$ transition from HOMO-3 to LUMO.

Rheological measurements

Effect of surfactant concentration on apparent viscosity

The effect of surfactant concentration (0.001–0.020 g/cc) on the apparent viscosity of IO slurry is shown in Figure 6. As per the plot, the slurry viscosity was significantly reduced by adding the aqueous extract of *Colocasia esculenta* (L.) Schott leaves. The surfactant molecules coated on the IOP surface which results dispersion due to formation of effective barrier between the IO particles. This will reduce the solid particle agglomeration to stabilise the slurry. With increase in surfactant concentration, the viscosity of IOS reduced sharply from ~1145 to ~550 mPa.s and there after no further substantial viscosity reduction was observed.

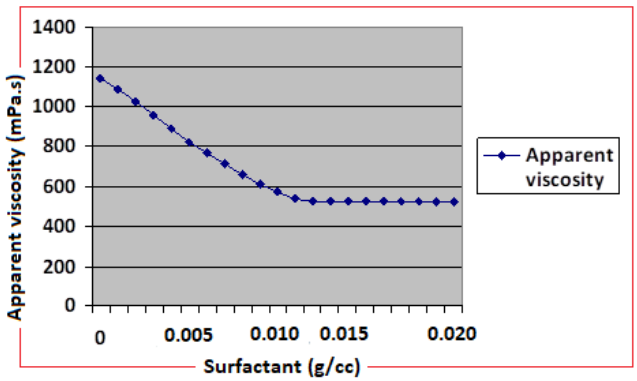

Figure 6. Plot of surfactant concentration vs apparent viscosity.

Effect of IO concentration on apparent viscosity

The apparent viscosity of IOS is crucial for its pipeline transportation. Figure 7 shows the effect of IO concentration on apparent viscosity of the studied IOS. The apparent viscosity of the studied IOS increases with increase in IO concentration due to particle–particle interaction. At higher concentration, the solid particle agglomeration results greater viscosity of the slurry. The apparent viscosity of the IOS gradually increases with increase in IO concentration. The apparent viscosity of the slurry sudden rises above 70% iron concentration (580 mPa.s) and reaches 850 mPa.s at 75% iron after which it may not be suitable for pipeline transportation. The graph suggests that solid content between 50% to 70% possess good fluidity and suitable for pipeline transportation. The effect of temperature on apparent viscosity of IOS at a concentration of 60% is also studied. The study suggested that the apparent viscosity of the slurry decreases with rise in temperature.

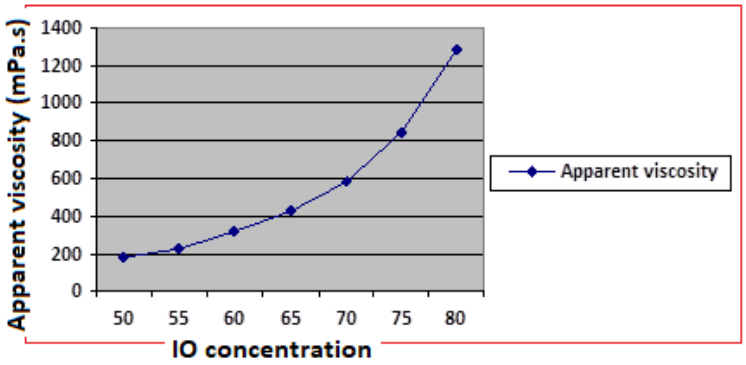

Figure 7. Plot of IO concentration vs apparent viscosity.

Rheological behaviour of IOS

The variation of shear stress with shear rate at different IO concentrations (60% and 70%) is shown in Figure 8. For a very low-concentration slurry, a straight line passing through the origin will be obtained for the shear stress vs shear rate plot. In the presence of aqueous extract of *Colocasia esculenta* (L.) Schott, the IOS displayed a linear relation between shear stress and shear rate, which indicates the non-Newtonian Bingham plastic model [10-12]. The applied shear rate must overcome the yield stress for the free flow of the slurry. From the plot, it is confirmed that the yield stress value increases significantly with the increase of IO concentration due to the strong agglomeration of iron ore particles at higher concentration.

$\tau = \tau 0 + \gamma\eta$

where, τ is shear stress, γ is applied shear rate, τ0 is yield stress and η is the Bingham viscosity.

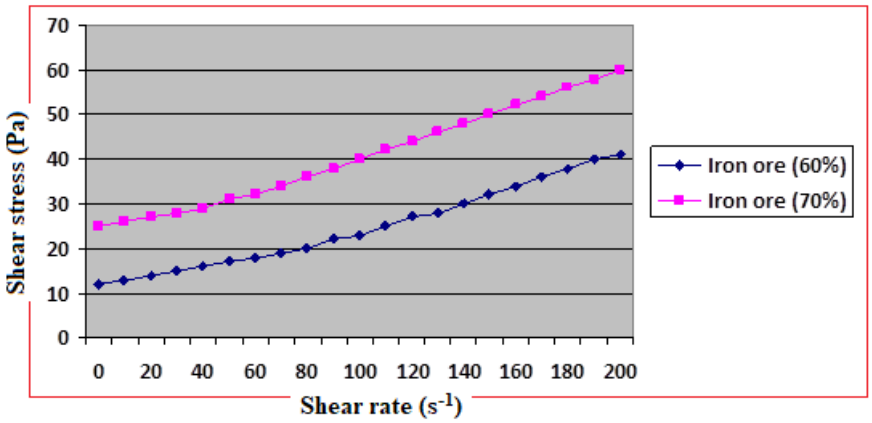

Figure 8. Plot of shear stress versus shear rate of IOS in the presence of *Colocasia esculenta* (L.) Schott.

Effect of shear rate on apparent viscosity

It is essential to understand the effect of shear rate on the apparent viscosity of IOS for its economical pipeline transportation. The variation of shear rate (10 to 200 s^{-1}) with apparent viscosity of the slurry at IO concentration 60% to 70% was studied. As per the plot, the apparent viscosity of the slurry decreases with rise of shear rate. The slurry with 60% IO concentration displayed lowest values of apparent viscosity and may be economical for its pipeline transportation.

Mechanism of stabilization of IO slurry

We know metal oxides are usually insoluble in water except few which are sparingly soluble in water. The surface of anhydrous hematite (Fe_2O_3) is slightly hydrophobic in nature at natural pH but the surface becomes hydrophilic when hydroxylation occurs at alkaline pH [24]. As reported, the saponin molecules are amphiphilic in nature. Due to this, in aqueous solution, the hydrophilic part of the saponin orientated towards the water molecules and the hydrophobic part away from the water molecules. This reduces the surface tension of water [25]. The solubility of IO increased when aqueous extract of *Colocasia esculenta* (L.) Schott is added to it. It is further suggested that the hydrophilic part of the surfactant is attached to the IO surface [26] and results greater solubility due to its micellization behavior (Figure 9).

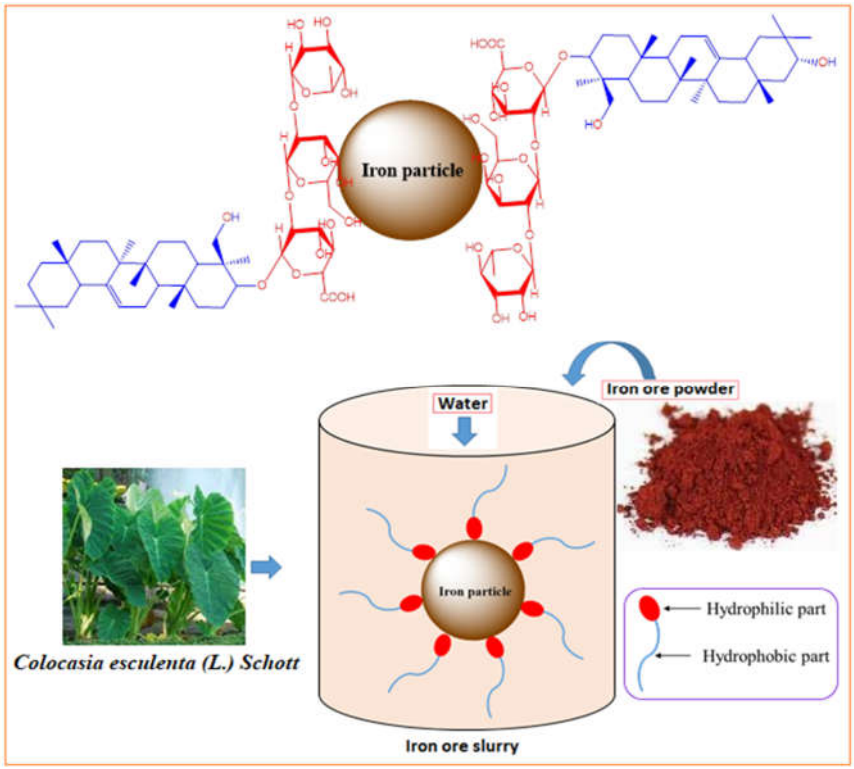

Figure 9. Illustration for the stabilization of IO slurry.

CONCLUSION

The rheological behaviour of the prepared IO slurry with concentration range of 50–70% by mass was investigated. The slurry was stabilised by adding a novel bio-surfactant extracted from *Colocasia esculenta* (L.) Schott. The aqueous extract of *Colocasia esculenta* (L.) Schott is used for the first time to stabilise IOS. Based on the density functional theory M06-2X/6-31G(d,p) method, we have found that the saponin molecule has 6.41 eV energy gap between HOMO/LUMO and the molecular charge distribution range of $-8.124e^{-2}$ to $8.124e^{-2}$. The MEP surface shows the possible nucleophilic attack on the methyl group whereas electrophilic at carboxylic functional group. Moreover, the electronic absorption spectra reveals the $\pi \rightarrow \pi^*$ transition in the UV region. The aqueous extract of *Colocasia esculenta* (L.) Schott enhanced the solubility of IO in the slurry. Further, the bio-surfactant reduced the viscosity of the slurry as the surfactant molecules coated well on the surface of IO particles. The results of XRF, XRD, SEM and EDS analysis also matches with the above findings. The rheological parameters suggested non-Newtonian flow behaviour. The stabilisation and transportation of IO slurry by using aqueous extract of *Colocasia esculenta* (L.) Schott leaf (an organic waste) may be an economic and eco-friendly alternative mode of transportation.

ACKNOWLEDGMENTS

All authors acknowledge their respective universities.

REFERENCES

1. Jacyna, M.; Wasiak, M.; Lewczuk, K.; Karoń, G. Noise and environmental pollution from transport: decisive problems in developing ecologically efficient transport systems. *J. Vibroengineering* **2017**, 19, 5639-5655.
2. Stojic, N.; Pucarevic, M.; Stojic, G. Railway transportation as a source of soil pollution. *Transp. Res. D: Transp. Environ*. **2017**, 57, 124-129.
3. Mohapatra, R.K.; Das, P.K.; Sharun, K.; Tiwari, R.; Mohapatra, S.R.; Mohapatra, P.K.; Behera, A.; Acharyya, T.; Kandi, V.; Zahan, K.-E.; Natesan, S.; Bilal, M.; Dhama, K. Negative and positive environmental perspective of COVID-19: Air, water, wastewater, forest, and noise quality. *Egypt. J. Basic Appl. Sci.* **2021**, 8, 364-384.
4. Das, S.N.; Biswal, S.K.; Mohapatra, R.K. Recent advances on stabilization and rheological behaviour of iron ore slurry for economic pipeline transportation. *Mater. Today: Proc.* **2020**, 33, 5093-5097.
5. Indian Bureau of Mines, Government of India Ministry of Mines, Slurry transportation in Indian mines, **2001**. Available at: https://ibm.gov.in/writereaddata/files/10072016172218slurry%20pdf.pdf
6. Senapati, P.K.; Pothal, J.K.; Barik, R.; Kumar, R.; Bhatnagar, S.K. Effect of particle size, blend ratio and some selective bio-additives on rheological behaviour of high-concentration iron ore slurry. Jewell, R.J.; Fourie, A.B. (Eds.), *Paste 2018: Proceedings of the 21st International Seminar on Paste and Thickened Tailings*, Australian Centre for Geomechanics, Perth, **2018**, 227-238.
7. Jennings Jr., H.Y. Transporting iron ore slurries, United States Patent, Appl. No.: 655,355, Filed: Feb. 5, **1976**.
8. Macía, Y.M.; Pedrera, J.; Castro, M.T.; Vilalta, G. Analysis of energy sustainability in ore slurry pumping transport systems. *Sustainability* **2019**, 11, 3191.
9. Das, S.N.; Biswal, S.K.; Mohapatra, R.K. Exploring the role of a bio-surfactant on the stabilization of high concentrated iron ore slurry, *RASAYAN J. Chem*. **2023**, 16, 1319-1325.

10. Gupta, C.; Kumar, S. Characterization and stabilization of iron ore suspension and influence of the mixture of natural additive Sapindus mukorossi and SDS on the slurryability. *J. Dispers. Sci. Technol*. **2023**, DOI: 10.1080/01932691.2023.2212752.
11. Behari, M.; Mohanty, A.M.; Das, D. Influence of a plant-based surfactant on improving the stability of iron ore particles for dispersion and pipeline transportation. *Powder Technol*. **2022**, 407, 117620.
12. Behari, M.; Mohanty, A.M.; Das, D. Insights into the transport phenomena of iron ore particles by utilizing extracted bio-surfactant from *Acacia concinna* (Willd.) Dc. *J. Mol. Liq*. **2023**, 382, 121974.
13. Das, D.; Pattanaik, S.; Parhi, P.K.; Mohapatra, R.K.; Jyothi, R.K.; Lee, J.-Y.; Kim, H.I. Stabilization and rheological behavior of fly ash−water slurry using a natural dispersant in pipeline transportation. *ACS Omega* **2019**, 4, 21604-21611.
14. Routray, A.; Senapati, P.K.; Padhy, M.; Das, D.; Mohapatra, R.K. Effect of mixture of a non-ionic and a cationic surfactant for preparation of stabilized high concentration coal water slurry. *Int. J. Coal Prep. Util*. **2022**, 42, 925-940.
15. Das, D.; Mohapatra, R.K.; Belbsir, H.; Routray, A.; Parhi, P.K.; El-Hami, K. Combined effect of natural dispersant and a stabilizer in formulation of high concentration coal water slurry: Experimental and rheological modelling. *J. Mol. Liq*. **2020**, 320, 114441.
16. Mohapatra, R.K.; Das, D.; Behera, U.; Das, S.N.; Mohanty, A.; Mahal, A.; El-ajaily, M.M. Generation of Fly ash and Its Surface Modification for Pipeline Transportation. Chapter: 5, (Chemical Modification of Solid Surfaces by the Use of Additives, edited by R. K. Mohapatra, D. Das, M. Azam). **2021**, 94-109. DOI: 10.2174/9789815036817121010008.
17. Routray, A.; Kar, P.; Nayak, N.; Mohapatra, R.K.; Mustakim, S.M.; Das, D. Improvement in the Flow Behavior of Coal–Water Slurry Using Surfactant Mixture. Chapter: 3, (Chemical Modification of Solid Surfaces by the Use of Additives, edited by R.K. Mohapatra, D. Das, M. Azam). **2021**, 44-59. DOI: 10.2174/9789815036817121010006.
18. Frisch, M.J.; Trucks, G.W.; Schlegel, H.B.; Scuseria, G. E.; Robb, M.A.; Cheeseman, J.R.; Scalmani, G.; Barone, V.; Mennucci, B.; Petersson, G.A.; Nakatsuji, H.; Caricato, M.; Li, X.; Hratchian, H.P.; Izmaylov, A.F.; Bloino, J.; Zheng, G.; Sonnenberg, J.L.; Hada, M.; Ehara, M.; Toyota, K.; Fukuda, R.; Hasegawa, J.; Ishida, M.; Nakajima, T.; Honda, Y.; Kitao, O.; Nakai, H.; Vreven, T.; Montgomery Jr., J.A.; Peralta, J.E.; Ogliaro, F.; Bearpark, M.; Heyd, J.J.; Brothers, E.; Kudin, K.N.; Staroverov, V.N.; Kobayashi, R.; Normand, J.; Raghavachari, K.; Rendell, A.; Burant, J.C.; Iyengar, S.S.; Tomasi, J.; Cossi, M.; Rega, N.; Millam, J.M.; Klene, M.; Knox, J.E.; Cross, J.B.; Bakken, V.; Adamo, C.; Jaramillo, J.; Gomperts, R.; Stratmann, R.E.; Yazyev, O.; Austin, A.J.; Cammi, R.; Pomelli, C.; Ochterski, J.W.; Martin, R.L.; Morokuma, K.; Zakrzewski, V.G.; Voth, G.A.; Salvador, P.; Dannenberg, J.J.; Dapprich, S.; Daniels, A.D.; Farkas, Ö.; Foresman, J.B.; Ortiz, J.V.; Cioslowski, J.; Fox, D.J. Gaussian 16, Wallingford, CT. Gaussian 16 (Revision A.03). **2016**. https://gaussian.com/citation/.
19. Zhao, Y.; Truhlar, D.G. The M06 suite of density functionals for main group thermochemistry, thermochemical kinetics, noncovalent interactions, excited states, and transition elements: two new functionals and systematic testing of four M06-class functionals and 12 other functionals. *Theor. Chem. Acc*. **2008**, 120, 215-241.
20. Kumar, M.; Ansari, M.; Ansari, A. Electronic, geometrical and photophysical facets of five coordinated porphyrin N–heterocyclic carbene transition metals complexes: A theoretical study. *Spectrochim. Acta Part A Mol. Biomol. Spectrosc*. **2023**, 284, 121774.
21. Kumar, M.; Gupta, M.K.; Rizvi, M.A.; Ansari, A. Electronic structures and ligand effect on redox potential of iron and cobalt complexes: a computational insight. *Struct. Chem*. **2023**. https://doi.org/10.1007/s11224-022-02119-3.

22. Das, D.; Sarangi,_A.K.; Mohapatra,_R.K.; Parhi, P.K.; Mahal,_A.; Sahu,_R.; Zahan, K.-E. Aqueous extract of Shikakai; a green solvent for deoximation reaction: Mechanistic approach from experimental to theoretical. *J. Mol. Liq*. **2020**, 309, 113133.
23. Neese, F. Software update: the ORCA program system, version 4.0. *WIREs Comput. Mol. Sci.* **2018**, 8. https://doi.org/10.1002/wcms.1327.
24. Shrimali, K.; Jin, J.; Hassas, B.V.; Wang, X.; Miller, J.D. The surface state of hematite and its wetting characteristics. *J. Colloid Interface Sci*. **2016**, 477, 16-24.
25. Rai, S.; Acharya-Siwakoti, E.; Kafle, A.; Devkota, H.P.; Bhattarai, A. Plant-derived saponins: A review of their surfactant properties and applications. Sci. **2021**, 3, 44. https://doi.org/10.3390/sci3040044.
26. Patra, A.S.; Makhija, D.; Mukherjee, A.K.; Tiwari, R.; Sahoo, C.R.; Mohanty, B.D. Improved dewatering of iron ore fines by the use of surfactants. *Powder Technol*. **2016**, 287, 43-50.